



Swansea University
Prifysgol Abertawe



Cronfa - Swansea University Open Access Repository

This is an author produced version of a paper published in :
Applied Surface Science

Cronfa URL for this paper:
<http://cronfa.swan.ac.uk/Record/cronfa31979>

Paper:

V., K., Prakash, K., Rajesh, R., Rammasamy, D., Selvaraj, N., Yang, T., Prabakaran, B. & Jothi, S. (2017). Electro deposition of r-GO/SiC nano-composites on Magnesium and its Corrosion Behavior in Aqueous Electrolyte. *Applied Surface Science*
<http://dx.doi.org/10.1016/j.apsusc.2017.02.082>

This article is brought to you by Swansea University. Any person downloading material is agreeing to abide by the terms of the repository licence. Authors are personally responsible for adhering to publisher restrictions or conditions. When uploading content they are required to comply with their publisher agreement and the SHERPA RoMEO database to judge whether or not it is copyright safe to add this version of the paper to this repository.
<http://www.swansea.ac.uk/iss/researchsupport/cronfa-support/>

Accepted Manuscript

Title: Electro deposition of r-GO/SiC nano-composites on Magnesium and its Corrosion Behavior in Aqueous Electrolyte

Authors: V. Kavimani, K. Soorya Prakash, R. Rajesh, Devaraj Rammasamy, Nivas Babu Selvaraj, Tao Yang, Balasubramanian Prabakaran, Sathiskumar Jothi



PII: S0169-4332(17)30444-0
DOI: <http://dx.doi.org/doi:10.1016/j.apsusc.2017.02.082>
Reference: APSUSC 35191

To appear in: *APSUSC*

Received date: 4-11-2016
Revised date: 5-2-2017
Accepted date: 10-2-2017

Please cite this article as: Kavimani V., K.Soorya Prakash, R.Rajesh, Devaraj Rammasamy, Nivas Babu Selvaraj, Tao Yang, Balasubramanian Prabakaran, Sathiskumar Jothi, Electro deposition of r-GO/SiC nano-composites on Magnesium and its Corrosion Behavior in Aqueous Electrolyte, *Applied Surface Science* <http://dx.doi.org/10.1016/j.apsusc.2017.02.082>

This is a PDF file of an unedited manuscript that has been accepted for publication. As a service to our customers we are providing this early version of the manuscript. The manuscript will undergo copyediting, typesetting, and review of the resulting proof before it is published in its final form. Please note that during the production process errors may be discovered which could affect the content, and all legal disclaimers that apply to the journal pertain.

Electro deposition of r-GO/SiC nano-composites on Magnesium and its Corrosion Behavior in Aqueous Electrolyte

V. Kavimani¹, K. Soorya Prakash¹, R.Rajesh², Devaraj Rammasamy³, Nivas Babu Selvaraj⁴, Tao Yang³,
Balasubramanian Prabakaran⁵, Sathiskumar Jothi^{6*}

¹Department of Mechanical Engineering, Anna University, Regional Campus, Coimbatore-641046, TN, India.

²Department of Nanotechnology, Anna University, Regional Campus, Coimbatore-641046, TN, India.

³Centre for Mechanical Technology and Automation, Department of Mechanical Engineering, University of Aveiro,
3810 193, Aveiro, Portugal.

⁴Department of Materials and Ceramics Engineering, CICECO, University of Aveiro, 3810-193 Aveiro, Portugal.

⁵Mahindra Aerospace, Aircraft Business, Manufacturing Unit, 43 Airfield Road Traralgon VIC 3844, PO Box 881
Morwell VIC 3840, Australia.

⁶College of Engineering, Swansea University, Singleton Park, Swansea, SA2 8PP, UK.

*s.jothi@swansea.ac.uk

Highlights for review

- Reduced graphene oxide (r-GO) was synthesized using modified hummer method.
- Reduced graphene oxide (r-GO)/Silicon Carbide (SiC) composite were coated on Mg Strip using electro deposition.
- Nanocomposite were characterized using Physio-chemical method.
- Surface morphology of coated composites was analyzed using SEM/EDAX.
- Corrosion study was carried out on the uncoated and coated Mg.

Abstract:

In this paper a detailed investigation for corrosion behavior of magnesium substrate electrodeposited differently by nanoparticles like Reduced Graphene Oxide (r-GO synthesized through Modified Hummer's Method), Silicon Carbide (SiC– mechanically alloyed) and also r-GO/SiC nanocomposites (dispersed through ultrasonication process) as coating materials for varying time period was done. Synthesized nanocomposite was characterized through various physio-chemical techniques and confirmation of the same was carried out. Surface morphology of the developed set of specimens was scrutinized through SEM and EDAX which establishes a clean surface coating with minimal defects attainment through electro deposition technique. Electrochemical corrosion behavior for the magnesium substrates coated with r-GO, SiC, r-GO/SiC for 5 and 10 minute coating time period was conceded over in 0.1 M of NaCl and Na₂SO₄ aqueous solution using Tafel polarization and then compared with a pure magnesium substrate. r-GO/SiC nanocomposite coated magnesium substrate showcased a drastic breakthrough in corrosion resistance when compared with other set of specimens in aqueous medium. Delamination behavior for the same set of specimens was carried and the r-GO/SiC nanocomposite coated magnesium exposed a minimum delamination area accounting to the hydrophobic property of graphene and the binding effect of SiC nano particles.

Keywords: Reduced Graphene Oxide, r-GO/SiC nano-composites, Corrosion resistance, Magnesium, Silicon Carbide, Electro-deposition.

1. Introduction:

Magnesium (Mg) considered to be one of the lightest structural metal has emerged as a material of lead focus by researchers worldwide in lieu of its low density with better strength to weight ratio while compared with that of commercially available steel and aluminum. Thus Mg promotes itself to be an eminent replacement in place of currently available rival materials that are used for structural applications in marine, automobile, and aerospace industries. Magnesium, its alloys and composites have the capability to decrease the component weight by ~35% and ~75% when compared to aluminum and iron based materials respectively that to with improvised fuel efficiency [1-3]. In practicality, relatively high vulnerability to corrosion in aqueous media (sea water) limits the use of Mg in brackish environment [4]. Corrosion resistance for Mg can be improved to a great extent by either alloying it with certain elements

or by the way of successful dispersion of high corrosion resistant ceramic particles; but both process may affect density as well as bulk properties of Mg that too in a negative mode [5-6]. These demerits prompted many researchers to consider various protective treatments over the surface of alloys, metals including Mg that may result in enhancement of its surface properties including hardness, sensing properties, strength, corrosion resistance etc. without affecting any of its bulk properties, affects the hydrogen diffusion properties & surface microstructural morphology, reduces the hydrogen induced cracking & degradation and hydrogen embrittlement [7-12]. Amongst the availability, treatments such as anodization, chemical conversion, electrodeposition, solution-cast deposition and etc have been proved to be most effective [13-21]. Yet again, certain studies on surface treatment has conveyed an enhancement in corrosion protection of Mg-based alloys, it is obvious that corrosion rate of metals, alloys and Mg based alloy is evidently high in chlorine rich environment when compared with aluminum based alloys [10, 15, 22]. Headed by these formulations gathered through existing literatures, it is supposed to be the need of the hour to improve corrosion resistance and there by wider the application range of Mg and its alloys in aqueous environments like NaCl, Na₂SO₄, KCl etc. It is worthwhile to further augment that such hypothetical research undergone will definitely provide an opportunity to amplify the usage of Mg and its alloys in the field of marine to a great extent.

Electrodeposition, a well accepted low cost coating practice is apt for creating a thin layer over a material surface thereby providing a corrosion protective shield when exposed to corrosive environments [23-24]. Ceramic and carbon based materials are widely used to prevent corrosion and thus enhance the strength of material surface. Specifically, nano carbon is a material that has got great attention towards enhancing corrosion resistant characteristic of the base substrate due to its high surface area to volume ratio besides also possessing rich electronic, thermal and mechanical properties [25-27].

Reduced Graphene oxide (r-GO), a two-dimensional carbon sheet with various oxygenated functional groups possesses some unique properties such as chemical inertness, chemical stability and high surface area which are conspicuously diverse from those of graphene due to the existence of surface functional groups [28-29]. Owing to the presence of functional group, r-GO displays better properties and so for this reason it can be termed as hybrid composite coating. During corrosion, electrons flow from anode to cathode region

completing the corrosion reaction. When r-GO like nano sheets are coated over a substrate, it forms a thin layer such that a function of r-GO's high surface area is formed that constrains the flow of electrons from metal surface inhibiting the corrosion rate [30-31]. Carbon based nanoparticle experiences certain cons like agglomeration and high conductivity which limits the corrosion resistance behavior. In recent years, effectual research in r-GO particles is carried over by proficiently reinforcing it with metals and ceramic nanoparticles like Ni, Cu, SiC, Al₂O₃, ZrB₂ etc for improving the mechanical and chemical properties of material surface by means of composite coatings and metal matrix composites [32-34]. Similarly, Silicon Carbide (SiC) increase significant tribological properties when used as reinforcement with r-GO, likewise addition of Al₂O₃ improves the electrical conductivity of r-GO [35]. Besides r-GO, r-GO based hybrid nanocomposite is established as a type protective coating to reduce oxidation on metals in corrosive environment like saline water [36]. Certain works paves light to the successful treatment of graphene and SiC particles as coating materials so as to strengthen many other appropriate materials.

P.Wang et al. prepared graphene by electrochemical exfoliation method with constant voltage of 10 V and a super hydrophobic coating over Al6061 alloy was developed so as to study its self cleaning and anticorrosion properties [37]. C.Chen et al. developed graphene based polymer coating over Q235 steel and wear and corrosion properties were investigated. Results concluded an optimistic approach in wear and corrosion behavior, however the dispersion of graphene sheets into polymer was found to be difficult [38]. A primer coating based on graphene with Poly Vinyl Butyral (PVB) was developed by Glover et al. to deduce the corrosion rate in irons and findings state as introduction of GNPs reduce coating's delamination rate [39].

Mg alloy was coated with graphene oxide through Plasma Electrolytic Oxidation (PEO) by J. Zhao et al. and it was confirmed that addition of GO upto 2g/l improves corrosion resistance. It was also concluded that GO incorporation through PEO process can enhance the microstructure compactness and reduce the porosity of coatings [40]. AISI 1045 steel was coated with SiC through cladding, mechanical and corrosive behavior of the same was investigated by C. Zhang et al. and results infer a reduction in porosity and corrosion values with addition of SiC nano particles besides an increment in hardness and wear resistance value [41].

Graphene nickel oxide coating through electrodeposition technique was carried out by Z. Xue et al. and nil agglomeration was observed [42]. AZ31B alloy was coated with SiC nano particles through micro arc oxidation methodology in which mechanical and corrosion resistance was found improvised. SiC nano particles coated through micro arc oxidation facilitates development of passive zone [43]. Ni-W-SiC coating over mild steel was carried out by S. Singh et al. through pulse electro deposition and results authenticated that SiO₂ acts as barrier for initiation and development of corrosion [44]. AISI 304 stainless steel substrate was coated with synthesized r-GO by J. Mondal et al. and the corrosion behavior analysis established an increased life time in substrate [45]. PEO method was experimented by Mingo et al. to coat SiC composite coating over AZ91 alloy and results depicted an increased corrosion and wear resistance with introduction in SiC fractions [46].

Hence this present work focuses on the enhancement of corrosion resistance of Mg by nano coating (r-GO/SiC) using linear electrodeposition technique. procedurally it is followed by synthesis and exfoliation of chemically reduced Graphene Oxide (r-GO) through Modified Hummer's Method. On further, r-GO is coated on Mg strip with different combinations, such as r-GO, SiC and r-GO/SiC at different time intervals. Corrosion behavior of r-GO, SiC, r-GO/SiC coated Mg strip was studied in 0.1M NaCl and Na₂SO₄ solution and then evaluated by performing Tafel polarization.

2. Experimental procedure:

2.1 Synthesis of r-GO Powder:

For the synthesis of r-GO and coating deposition, analytical grade chemicals were purchased and used without any purification. Pure graphite flakes as been considered for the synthesis of r-GO which was purchased directly from Otto chemicals Ltd. Acquirement of chemicals such as magnesium chloride (MgCl₂), potassium permanganate (KMnO₄), hydrogen peroxide (H₂O₂), silicon carbide (SiC) were perused from Merck, and hydrochloric acid (HCl), sulphuric acid (H₂SO₄) and hydrazine hydrate (NH₂.NH₂.H₂O) from Fishers Scientific. Thus purchased SiC measured at 40µ size and further reduced to ~ 0.04 µm by the way of ball milling.

Modified Hummers method [47] was used to prepare r-GO. In brief, Graphite flakes (1g) was added to beaker containing H₂SO₄ (40 ml) and the mixture was stirred for 2h in ice

bath besides maintaining at the temperature below 5°C. KMnO_4 (6 g) is added slowly into the mixture and temperature is maintained below 10°C. After 2h of stirring 90 ml of distilled water is added slowly and now with controlled temperature below 35°C, a gel like solution is formed. Then this solution is stirred for 2h into which 240 ml of distilled water is added and further allowed to be get stirred at a vigorous speed. Into this combination, 5ml of H_2O_2 is added so as to complete the oxidation reaction and as an outcome a bright yellow solution is formed confirming for GO formation. It was further allowed to settle down, diluted, filtered, washed with distilled water and 10% HCl and then dried so as to acquire purified GO particles. The dried GO powder is chemically reduced by hydrazine hydride at 80°C in order to obtain r-GO.

2.2. Sample preparation for corrosion studies:

For electrochemical corrosion test, a pure Mg strip with dimensions of 2mm width, 2mm thickness and 50mm height was employed. Mg strip subjected to electrodeposition is polished in accord to metallographic standards instituting SiC emery sheets of different grades and the subjected strip is cleaned with distilled water and ethanol respectively so as to remove any of the debris present over the surface. r-GO, SiC and r-GO/SiC nanocomposite coating was done by linear electrodeposition technique and hence firstly 5mg of MgCl_2 was dissolved in 50 ml of aqueous ethanol and then appropriate amount of r-GO nanosheets were dispersed into the solution and sonicated for about 30 minutes. Polished Mg strip is immersed into the resultant solution and 12V potential was applied between the electrodes for 5 minutes. Finally, r-GO coated Mg strip was allowed to set air dried at 80°C for 12h. The same procedure was carried out for depositing SiC and r-GO/SiC nanocomposites above the Mg substrate. In this context to study and compare the coating deposition with respect to time, similar another sample for an increased deposition time of 10 minutes was fabricated; yet again all sorts of experimentations were carried over for evaluation.

2.3 Material Characterization:

The phase and crystalline nature of the prepared samples were analyzed by powder X-ray diffractometer (PXRD) (BRUKER D8 ADVANCE). The samples were scanned over the 2θ range of 10° to 80° angle at room temperature (298 K). The observed peak positions and

relative intensities of the powder pattern were identified in comparison to reference diffraction data. Surface morphology of coated samples was examined under scanning electron microscopy coupled with energy dispersive X-ray analysis (SEM-EDAX) (JEOL JSM-6610LV, Japan) operating at 20 kV. Raman spectra of prepared r-GO sample were obtained using a Raman spectrometer (Horiba-Jovin Yvon - LABRAM HR) confocal Raman systems equipped with an Nd:YAG laser. Raman spectra were recorded with a frequency of 514 nm as an excitation source used with a laser spot size of 1 mm. Identification of functional groups was done by Fourier Transform Infrared spectroscopy (FTIR, Spectrum GX, Perkin Elmer, USA.)

2.4 Electrochemical corrosion studies:

The corrosion behavior of coated Mg strip is exemplified using CHI604C workstation instrument. All electrochemical investigations were carried out at room temperature with a three electrode setup that are used as pertaining for corrosion studies; wherein the coated strip, platinum wire and saturated calomel are taken as working electrode, counter electrode and reference electrode respectively. For the materials corrosion behavior examined in electrolytes tafel polarization was carried out between -1.3 V to -1.8 V at a scan rate of 0.01 V/s and then all of the experiments were repeated for 5 times so as to confirm the exactitudes of the results.

3. Result and discussion:

3.1 XRD confirmation for r-GO

The crystalline nature and degree of exfoliation of the synthesized r-GO was studied by powder X-ray diffraction technique and the corresponding diffraction pattern is as shown in Fig.1. diffractogram, depicts for a broad peak at $2\theta=24.4^\circ$ corresponding to (002) plane of the graphite structure; a small peak at $2\theta=43.3^\circ$ of higher order reflections of (100) plane observed confirms for the retention of graphite structure after reduction process. In addition to this, a peak at $2\theta=12.4^\circ$ notified indicates the presence of disordered graphitized structure and also the formation of partially r-GO.

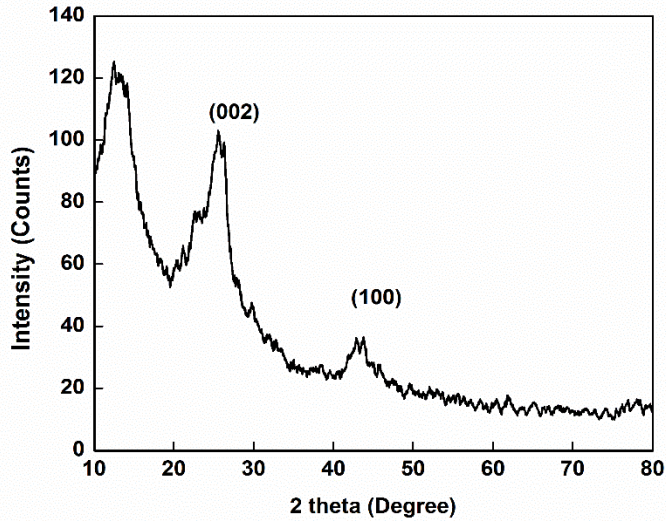


Fig. 1. XRD Patten of synthesis r-GO

3.2 Raman spectroscopy studies for r-GO:

In order to inspect the worth of synthesized r-GO, Raman spectroscopy tests were performed and Fig. 2 shows the spectrum for the same with its G and D bands. From Raman spectrum, two characteristic peaks were observed at 1351 cm^{-1} and 1593 cm^{-1} corresponding to D band and G band respectively confirming to the lattice distortion. G band is the characteristic feature of carbon layer which corresponds to the tangential vibration of carbon atom and D band corresponds to defects in graphitic carbon. Intensity of G band being slightly higher than D band confirms for the retention of ordered graphitized material leading to poor conductivity of r-GO which in turn results in low corrosion density that could upturn corrosion resistance of coated substrate. The intensity ratio (I_D/I_G) between D and G band is 0.92. The increased D/G intensity ratio decreases the average size of sp^2 carbon domain upon any reduction in exfoliated GO [48-49].

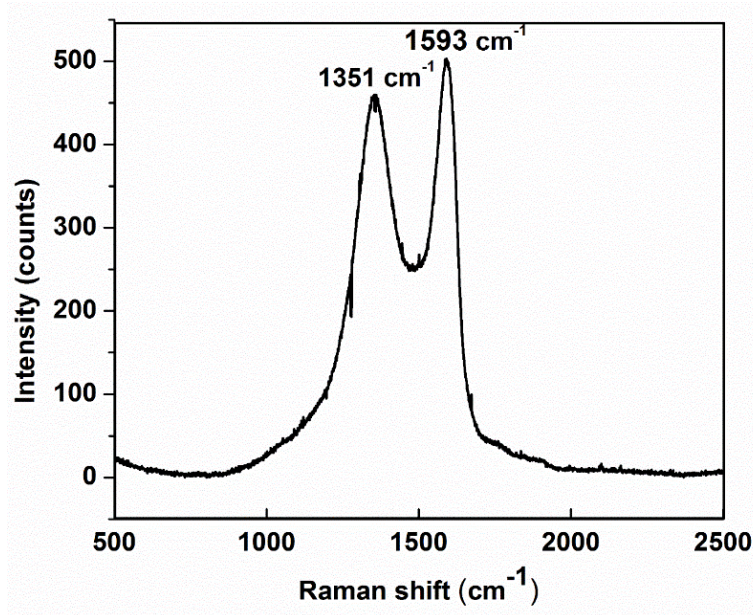


Fig.2. Raman spectrum of synthesis r-GO

3.3 Fourier Transform – infra red:

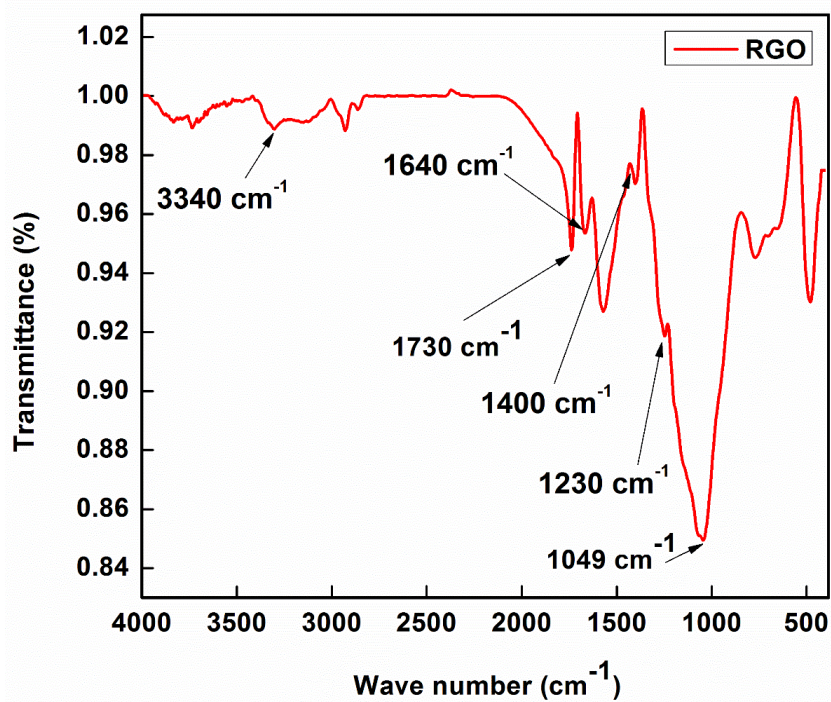


Fig. 3. FTIR spectroscopy of synthesis r-GO

The molecular vibration and functional groups of r-GO is studied by FTIR spectroscopy and the consequent results are as shown in Fig.3. Absorption peaks between $[1400 - 1650 \text{ cm}^{-1}]$ assign to aromatic C=C skeletal vibration of graphitic carbon; band at 1049 cm^{-1} attributes to C=O in carboxyl groups. Absorption band at 3340 cm^{-1} assigned to O-H group stretching vibration with oxygen contain group [50-51]. The strong absorption band at 1730 cm^{-1} arises due to C=O stretching vibration of COOH groups, the peak at 1640 cm^{-1} corresponds to C=C bending vibration and band of 1230 cm^{-1} sets assigned to epoxy CO stretching vibration. As well, the peak at 1400 cm^{-1} is attributed to C-O-H deformation vibration.

3.3 Microstructural studies for Nano composite coating:

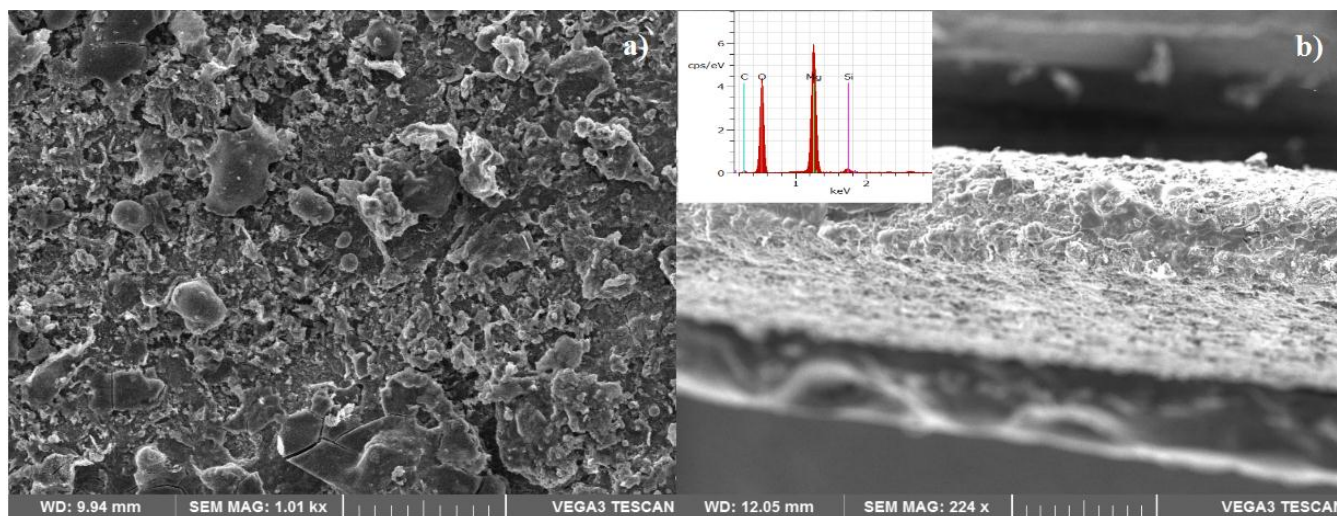
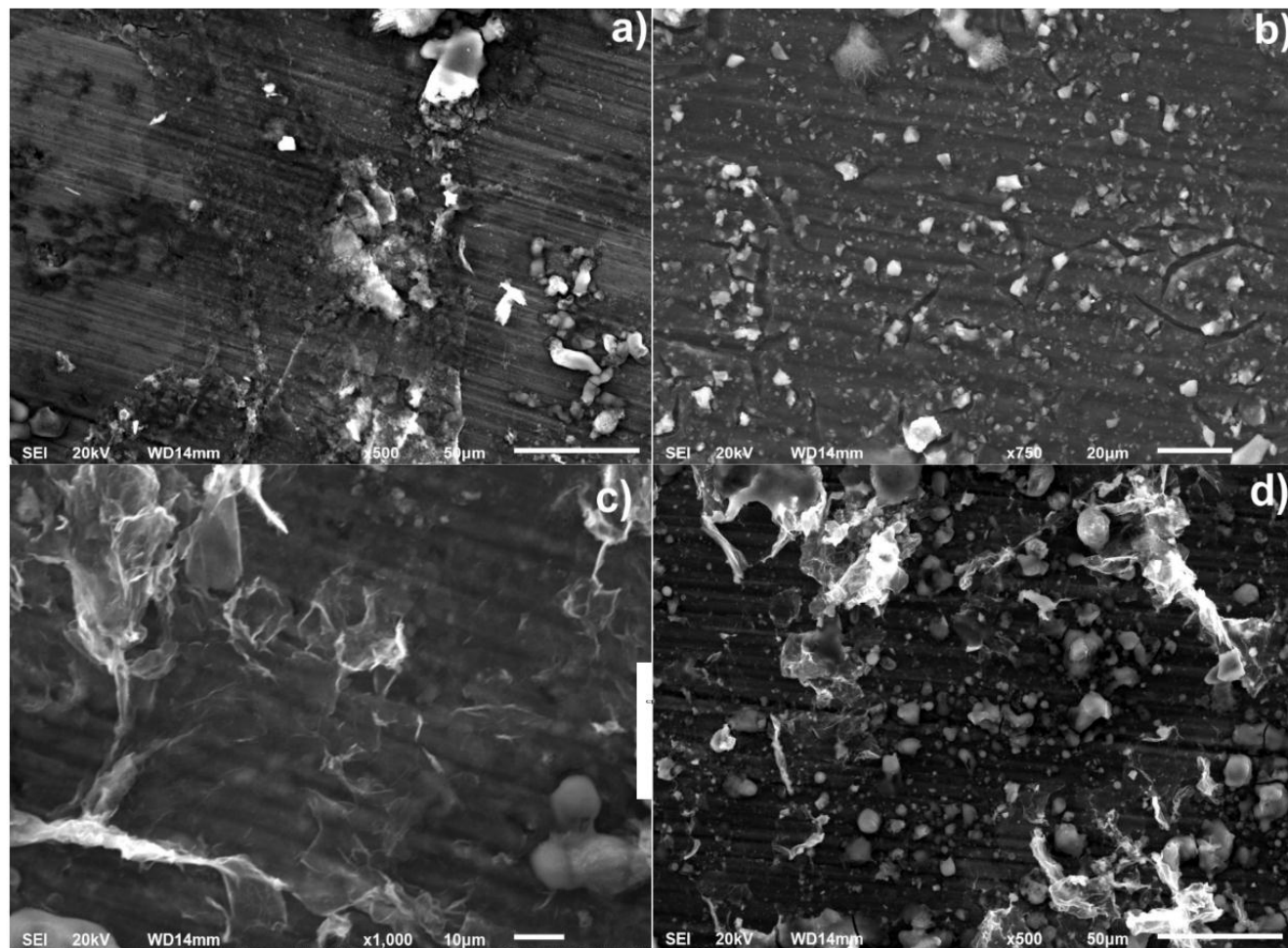


Fig.4. SEM micrographs: a) r-GO/SiC Coated surface b) EDAX r-GO/SiC of Coated surface

SEM micrographs for r-GO/SiC nanocomposite coated Mg substrate is demonstrated as Fig.4 (a-b) and a detailed insight through Fig. 4a states the clear distribution of r-GO and SiC particles over Mg substrate while considering Fig. 4b, the uniform deposition of nanoparticles as coating over Mg substrate can be observed. In addition to that, the layer formation also seems to be uniform and EDAX results of the same depicts the presence of carbon, magnesium, silicon and oxygen elements thereby confirming the presence of graphene nanosheets and SiC particles coated above Mg substrate.



**Fig. 5 SEM micrograph of corroded surface of a) Pure Mg b) SiC c) r-GO
d) r-GO/SiC coatings**

Surface morphologies for corroded surface of the coating are provided in Fig.5 (a–d), out of which Fig.5a displays the SEM morphologies of pure Mg strip after corrosion test wherein corroded surface can be easily notified. SEM micrographs for SiC coated Mg substrate after corrosion behavior portrayed as Fig.5b illustrates the crack formation over the strip supposed to be an after effect of corrosion mechanism and the presence of SiC particles over the surface is also visible. In the case of r-GO coating, SEM images as shown in Fig.5c demonstrate a chemically inert r-GO layers that protects Mg surface from the adversity of corrosive solution. Unfortunately, with increase in corrosion cycles, a peeling out of r-GO layers can be observed through the micrograph. So, to reduce the peeling out occurrence of these layers, novelty through introduction of SiC particles into r-GO nanosheets were carried

over bearing in mind the predictive reason that binding will definitely be created between Mg substrate and the coating material. Henceforth to support this theory, a clear cut examination done over SEM micrographs of the corroded Mg substrate surface coated with r-GO/SiC nanocomposites demonstrates for nil peeling out of r-GO layers. Also the presence of SiC particles amongst the layers can be witnessed through an eye as Fig. 5d.

3.5 Corrosion studies:

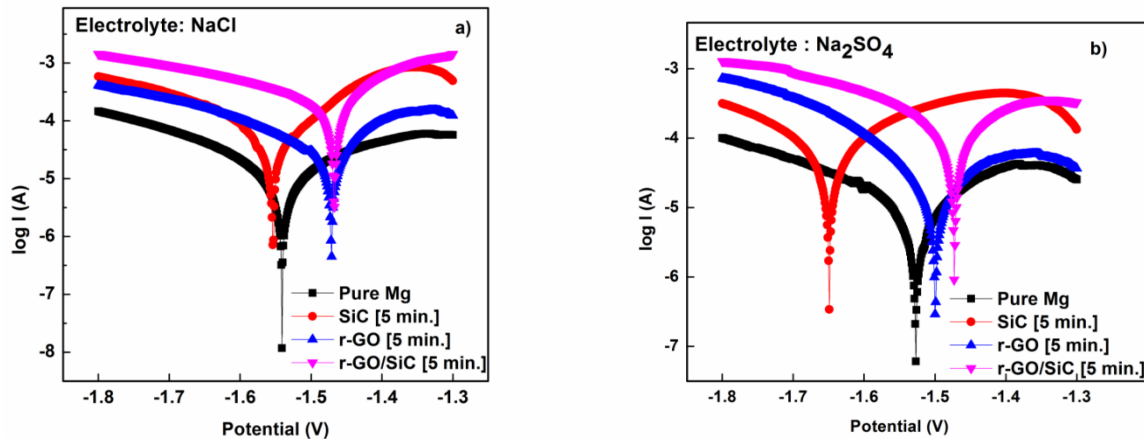
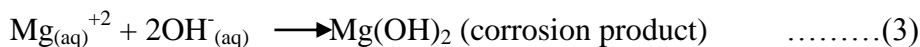
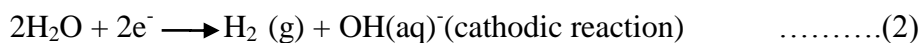
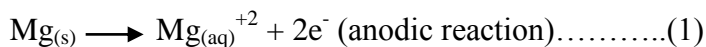


Fig.6. Comparative tafel plot for hybrid r-GO 5 minutes coated Mg strip in aqueous electrolyte.

Corrosion characterization of the coated Mg substrate was carried out and compared along with the values of pure Mg. Graphical representation of the same by means of Tafel plot are illustrated as Fig. 6(a-b) among which Fig.6a displays the electrochemical polarization plot for pure Mg and for coated Mg substrates in 0.1M NaCl electrolytic condition while Fig.6b describes the same for specimens exposed and duly tested for corrosion behavior under 0.1M Na₂SO₄ solution as electrolytic medium.

In aqueous electrolyte pure Mg undergoes the reaction as shown below [48]



Corrosion Rate (CR) was calculated by using corrosion current density,

$$CR = \frac{K i_{corr} EW}{d} \dots \dots \dots (4)$$

where, K is corrosion rate constant (milli-inch per year), EW is equivalent weight of Mg, d is material density, Polarization resistance (R_p) is calculated from Stearn–Geary equation[52] and are as represented in Table 1 and 2.

$$R_p = \frac{\beta_a \beta_c}{2.3 i_{corr} (\beta_a + \beta_c)} \dots \dots \dots (5)$$

Corrosion Current (i_{corr}), Corrosion Potential (E_{corr}), Anodic Tafel (β_a) and Cathodic Tafel (β_c) constants are calculated through curve fitting and are then tabulated for any further reference throughout the study.

From Tafel plot, the anodic Tafel constant (β_a) implies metal dissolution and cathodic Tafel shows hydrogen evolution. If hydrogen formation is high, then the cathodic current potential is more negative compared to corrosion potential likewise if metal oxidation is more than the anodic current potential is more positive when compared with that of corrosion potential.

With NaCl solution as electrolyte, results showcases a corrosion potential of -1.54 V, corrosion current density value $9.43 \mu\text{A}/\text{cm}^2$, corrosion rate 8.64 milli-inch per year (mpy) and Polarization Resistance (R_p) of 4384 ohm cm^2 for pure Mg strip which can very well be notified from Fig. 5a. Corrosion potential shifted from -1.54 V to -1.55 V towards cathodic region for SiC coated Mg substrate; its corrosion rate decreases from 8.54 mpy to 4.65 mpy and R_p value suddenly dips from $4384 \Omega\text{cm}^2$ to $725 \Omega\text{cm}^2$. Observations over results displayed a cathodic shift in the case of potential current but corrosion rate value tends to decrease which can be attributed to the cathodic nature of dispersed SiC particles and in addition to this SiC nano powders assist in the development of passive region thereby reducing corrosion rate [53]

Detailed analysis over the corrosion results of r-GO coated Mg strip in NaCl solution monitored for an anodic potential shift from -1.55V to -1.46 V, a reduction in corrosion rate from 5.02 mpy to 2.48 mpy and an increased R_p value from $725 \Omega\text{cm}^2$ to $1136 \Omega\text{cm}^2$. Inhibition of corrosion rate was attained when coated with r-GO which may be due to the chemical

inertness of r-GO nanosheets and its ability to act as a barrier inhibiting the penetration of corrosive electrolyte in to the metal substrate. Investigation over the corrosion behavior of Mg strip coated with r-GO/SiC nanocomposites showcased a cathodic shift in the case of potential from -1.46V to -1.47 V, reducing the corrosion rate from 2.48 mpy to 2.18 mpy and increasing R_p value from 1136 Ωcm^2 to 2049 Ωcm^2 . Mechanism behind reduction in corrosion rate in the case of r-GO/SiC nanocomposites coated specimen can be stated as delay in the crystal growth of the coating and attributes for an after effect of r-GO presence [54].

From these coated strips with various ceramic composites for a deposition time of 5 minutes, r-GO/SiC coated Mg strip, have good corrosion potential which move toward anodic region when compared with bare Mg strip and the former also exhibits high polarization resistance and lower corrosion rate. The same trend is seen in Na_2SO_4 solution, wherein we can observe that r-GO/SiC coated Mg strip have corrosion potential of -1.47 V which moves toward anodic region while compared with pure Mg strip. Also it has low corrosion rate of 1.20 mpy and high polarization Resistance of 4036 Ωcm^2 when compared to other coated strips. From Fig. 5b it can be noted that SiC coated Mg strip has corrosion potential of -1.64 V shifted toward cathodic region. It can be state that SiC particles trends to reduce the localized corrosion and further addition of SiC particle reduce the chance of corrosion area and hence improvise the corrosion resistance. r-GO coated strip has -1.49 V corrosion potential move toward anodic region which would further decrease the corrosion rate. Inhibiting efficiency of the coating can be calculated based on the corrosion current density [55] as shown in Eqn. (6)

$$\eta = \frac{i_{corr(bare)} - i_{corr(coating)}}{i_{corr(bare)}} \times 100 \dots \dots \dots (6)$$

From the above equation(6) the inhibiting efficiency of SiC coated strip is 27 %, r-GO coated strip have high inhibiting efficiency (73%) when compared with SiC coated strips. Meanwhile r-GO/SiC composite coated strip have better inhibiting efficiency of 85 %. Tafel plot confirms that r-GO/SiC coated Mg strip poses upright corrosion resistance in both NaCl and Na_2SO_4 aqueous solution. Corrosion parameters of coated samples as described above in NaCl and Na_2SO_4 solution are obtained from potential dynamic study as detailed in Table.1. and Table. 2.

Table.1. Corrosion parameter derived from Tafel plot for NaCl electrolyte for 5

minutes duration

Coating	Corrosion current density $I_{\text{corr}}(\mu\text{Acm}^{-2})$	Corrosion potential E_{corr} V (SCE)	Cathodic tafel constant $\beta_{\text{c}}(1/\text{V})$	Anodic tafel constant, $\beta_{\text{a}}(1/\text{V})$	Corrosion rate, V_{corr} ($\times 10^{-5}$ mpy)	Polarization Resistance $R_{\text{p}}(\Omega\text{cm}^2)$
Pure Mg	9.43	-1.54	5.71	4.79	8.64	4384
SiC	5.02	-1.55	4.96	6.95	4.65	725
r-GO	2.73	-1.46	5.29	9.22	2.48	1136
r-GO/SiC	2.38	-1.47	3.71	5.06	2.18	2049

Table. 2. Corrosion parameter derived from tafel plot for Na_2SO_4 electrolyte for 5 minutes duration

Coating	Corrosion current density $I_{\text{corr}}(\mu\text{Acm}^{-2})$	Corrosion potential $E_{\text{corr}}(\text{V})$	Cathodic tafel constant $\beta_{\text{c}}(1/\text{V})$	Anodic tafel constant, $\beta_{\text{a}}(1/\text{V})$	Corrosion rate,CR ($\times 10^{-5}$ mpy)	Polarization Resistance $R_{\text{p}}(\Omega\text{cm}^2)$
Pure Mg	8.24	-1.52	4.02	5.47	7.56	5552
SiC	6.02	-1.64	4.80	4.96	5.47	738
r-GO	2.30	-1.49	6.23	2.84	2.12	2073
r-GO/SiC	1.31	-1.47	4.803	3.38	1.20	4036

From calculated values the corrosion current density is low for r-GO/SiC coated strip which showcase low corrosion rate. As illustrated by Fig. 7a. it can be observed that r-GO/SiC has shifted toward anodic region while compared with r-GO coated strip demonstrating lower corrosion rate. From fig. 7b. it can be observed that SiC coated strip has high potential current than the hybrid coated strip.

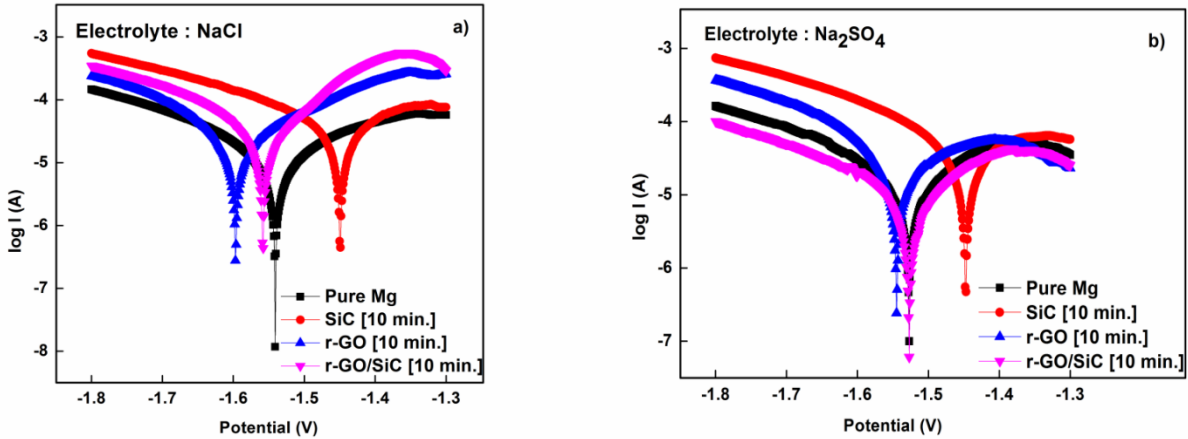


Fig.7. Comparative Tafel plot for hybrid r-GO 10 minutes coated Mg strip in aqueous electrolyte.

Mg strip with SiC ceramic coated for a deposition time of 10 minutes, exhibits a corrosion potential shift from -1.53 V to -1.44 V toward anodic region, corrosion rate decrease from 8.6 (mpy) to 4.64 mpy and R_p value decrease from $4384 \Omega \text{ cm}^2$ to $1410 \Omega \text{ cm}^2$. It can be explained that presence of SiC particle over the metal surface blocks the flow of faradic current. In case of r-GO coated Mg strip tested under the same testing conditions a shift in corrosion potential from -1.53V to -1.59 V towards cathodic region, can be experienced besides deducing its corrosion rate from 8.4 mpy to 1.93 mpy and increment in R_p value increases from $1410 \Omega \text{ cm}^2$ to $1854 \Omega \text{ cm}^2$ while comparing with SiC coated strips. This phenomenon illustrates that increasing the deposition time of r-GO on Mg strips in turn improves the corrosion resistance of the subjected specimen material. Likewise increase in the cathodic constant depicts for high hydrogen evolution and less value of anodic constant accounts for less metal oxidation.

Corrosion behavior of r-GO/SiC coated Mg strip immersed in NaCl solution exemplifies a cathodic shift in the case of corrosion potential which gets shifted from -1.53 V to -1.56 V, a decrease in corrosion rate from 8.64 mpy to 1.69 mpy and R_p value decrement from $1854 \Omega \text{ cm}^2$ to $1818 \Omega \text{ cm}^2$. In the case of samples coated for a coating period of 10 mins; r-GO/SiC coated Mg strip, have good corrosion potential which move toward anodic region when compared with base Mg strip. But r-GO coated Mg strip have high polarization resistance and low corrosion

rate. The above said property enhancement by the introduction of r-GO can be explained as the effect of unique structure offered by r-GO that in turn head to attain good impermeability. Increased deposition time of r-GO/SiC prompts for a considerable increase in corrosion resistance of the coated Mg strip immersed in NaCl.

Considering the corrosion behavior of specimens in Na_2SO_4 solution electrolytic condition, r-GO/SiC coated Mg strip exhibited a corrosion potential of -1.52 V which moves toward anodic region when compared with r-GO coated Mg strip, also it has low corrosion rate of 1.12 mpy but a lower polarization resistance of $3312 \Omega\text{cm}^2$. From Fig.6 (a-d). It is observed that corrosion potential of r-GO/SiC shifted more towards anodic region which inturn confirms the low corrosion rate of the sample. Tafel plot confirms that corrosion resistance of r-GO/SiC coated sample had better resistance in both 1+ ion and 2+ ions. Inhibiting efficiency of SiC coated strip is 51%, 70% for r-GO coated strip and r-GO/SiC coated strip has better inhibiting efficiency of 87%. The calculated kinetic corrosion parameter from the Tafel plot is shown in Table.3.and Table.4. The addition of SiC provides more corrosion resistance and thus may lead in SiC intercalate between the r-GO layers and increase the corrosion resistance behavior on Mg.

Table.3. Corrosion parameter derived from Tafel plot for NaCl for 10 minute duration

Coating	Corrosion current density $I_{\text{corr}}(\mu\text{Acm}^{-2})$	Corrosion potential $E_{\text{corr}}(\text{V})$	Cathodic tafel constant $\beta_{\text{c}}(1/\text{V})$	Anodic tafel constant, $\beta_{\text{a}}(1/\text{V})$	Corrosion rate, CR ($\times 10^{-5}$ mpy)	Polarization Resistance $R_{\text{p}}(\Omega \text{ cm}^2)$
Pure Mg	9.43	-1.53	5.71	4.79	8.64	4384
SiC	5.01	-1.44	3.53	2.61	4.64	1410
r-GO	2.11	-1.59	6.06	5.02	1.933	1854
r-GO/SiC	1.78	-1.56	5.66	5.02	1.69	1818

Table 4. Corrosion parameter derived from Tafel plot for Na₂SO₄ for 10 minute duration

Coating	Corrosion current density $I_{\text{corr}}(\mu\text{Acm}^{-2})$	Corrosion potential $E_{\text{corr}}(\text{V})$	Cathodic tafel constant $\beta_{\text{c}}(1/\text{V})$	Anodic tafel constant, $\beta_{\text{a}}(1/\text{V})$	Corrosion rate, CR ($\times 10^{-5}$ mpy)	Polarization Resistance $R_{\text{p}}(\Omega\text{cm}^2)$
Pure Mg	8.24	-1.51	4.02	5.47	7.56	5552
SiC	4.05	-1.44	5.37	1.30	4.13	1444
r-GO	2.51	-1.54	5.88	3.22	2.30	1900
r-GO/SiC	1.10	-1.52	5.76	4.97	1.12	3312

3.6 Linear Polarization Resistance:

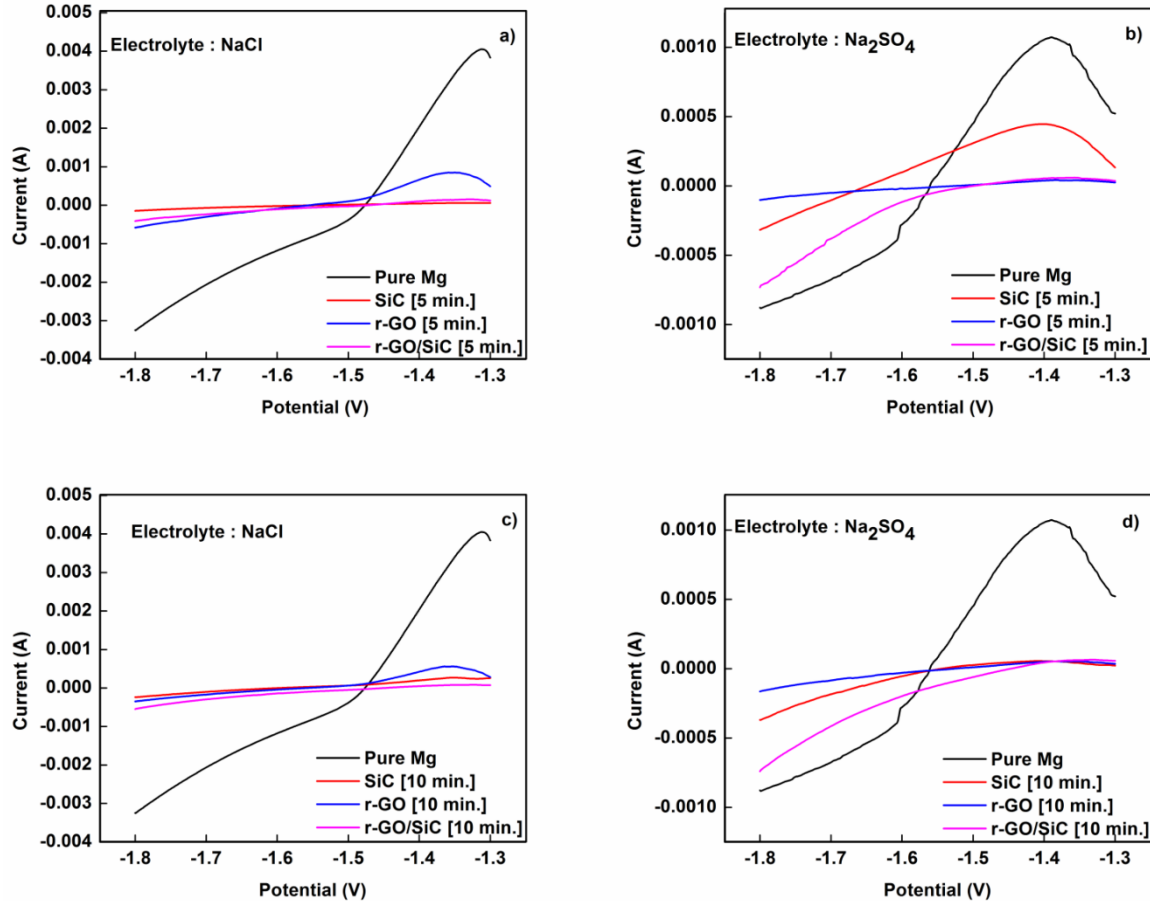


Fig. 8. Linear polarization resistance of coated samples in aqueous electrolyte.

Linear polarization resistance can be calculated by plotting potential Vs current and can be further manipulated using curve fitting method as show in Table 5. linear polarization resistance (LPR) chart are shown in Fig. 8 (a-d) for coated samples with different time interval. Increase in the value of LPR suggests high corrosion resistant of the material [56]. r-GO / SiC coated Mg strip posed high linear polarization resistance when compared with other samples. In aqueous NaCl solution LPR value for SiC coated strip is $484 \Omega \text{ cm}^2$ when coated for 5 minutes interval of time, yet LPR values increases to $1278 \Omega \text{ cm}^2$ while increasing the coating time up to 10 minutes, results of similitude were obtained in the case of Na_2SO_4 solution. Also when r-GO coated strip is dipped in electrolyte, the LPR value is observed as $757 \Omega \text{ cm}^2$ but increases to $939 \Omega \text{ cm}^2$ first by increasing the coating time. r-GO coated strip has higher LPR ($1384 \Omega \text{ cm}^2$) value in Na_2SO_4 but increasing the coating time result in decreasing LPR value drastically just because of r-GO (poor conductivity) thickness in coating. Likewise hybrid coating at 5 minutes interval

of time have yielded high LPR value ($2937 \Omega\text{cm}^2$) while comparing with that of 10 minute coated strip ($1036 \Omega\text{cm}^2$)

Table. 5. Linear Polarization Resistance of coated samples

Material	LPR ($\Omega \text{ cm}^2$)			
	NaCl		Na ₂ SO ₄	
	5 mins	10 mins	5 mins	10 mins
SiC	484	1278	492	1268
r-GO	757	939	1384	963
r-GO/SiC	2937	1036	3707	2211

3.7 Delamination Properties:

Delamination area is evaluated in order to specify the capacity of a coating to withstand in corrosion medium without peeling out from the substrate. Delamination area is calculated based on equation (7) [57] in which Specific polarization resistance, (R_p^0) is associated with the charge transfer behavior of the metal substrate, and can be estimated using the linear polarization of an uncoated sample of the substrate. The polarization test is conducted in 0.1M NaCl electrolyte. The value of R_p is assumed to be constant, and it is again assumed that the corroding environment of a coated sample is similar to that of an uncoated sample. Assumption made for the study explains that delamination area is equal to the corroded area on the metal surface.

$$\text{Delamination area (Da)} = (R_p^0) / R_p \text{ cm}^2 \dots \dots \dots (7)$$

Table. 6 Delamination area for coated samples.

Materials	Delamination area(Da) cm^2		
	24 hours	48 hours	72hours
ng (5 mi ns SiC	0.4241	0.785	0.913

Coating (10 mins)	r-GO	0.2114	0.347	0.825
	r-GO/SiC	0.1403	0.251	0.428
	SiC	0.4368	0.341	1.089
	r-GO	0.2574	0.485	1.103
	r-GO/SiC	0.1123	0.337	0.446

From Table.6.it can observed that at 24 hours of immersion, the corroded area is more for SiC coated strips and the r-GO/SiC coated strip have less delamination area of 0.143 cm². This may be the effect of better intercalation between the nanomaterials. And also found to remain for a longer time preventing from any further penetration of corrosive electrolyte into the coated substract. It can be notified that r-GO coated strip have minimal corroded area and hence once again proves for the hydrophobic tendency of the r-GO nano sheet. Likewise, 10 minutes coated r-GO/SiC has low delaminated area which proves the efficiency of material to prevent corrosion. It can be observed that for 48 and 72 hours of immersion the delamination area is lower for the composite coating thus illustrates the tendency of material to act as corrosion inhibitor. Da value is noticed to be lower for r-GO/SiC coating for both 5 and 10 minutes coating time intervals. This may be due to better bonding between the developed r-GO/SiC coatings and lower Da values indicates better peeling resistance of the coating

Conclusion:

In this work, reduced graphene oxide was synthesized by Modified Hummer's Method and deposited along with SiC over Mg surface using linear electrodeposition technique. The corrosion behavior of all coated metal strips is studied in 0.1 M NaCl and Na₂SO₄ solution using Tafel polarization measurements. Electrochemical measurements in two different aqueous electrolytes of NaCl and Na₂SO₄ reveals a sharp decrease in corrosion rate for r-GO/SiC composite coating and also it has better inhibited efficiency in both solutions. The excellent corrosion resistance in aqueous electrolytes suggests that r-GO/SiC composite coated Mg possess the potential for ready usage in marine applications.

Acknowledgements

Corresponding author Dr.Sathiskumar Jothi acknowledges the ASTUTE 2020 (Advanced Sustainable Manufacturing Technologies; Project number: 80814) which is part-funded by the European Regional Development Fund through the Wales Government and the participating Higher Education Institutions.

Reference :

- [1] Benjamin M. Wilkea, Lei Zhanga, Weiping Lib, Chengyun Ningb, Cheng-fu Chena, Yanhong Guc, Corrosion performance of MAO coatings on AZ31 Mg alloy in simulated body fluid vs. Earle's Balance Salt Solution, *App. Surf. Sci.* 363(2016), 328–337
- [2] J. Chen, Y. Song, D. Shan, E.-H. Modifications of the hydrotalcite film on AZ31 Mg alloy by phytic acid: The effects on morphology, composition and corrosion resistance Han, *Corros. Sci.* 74 (2013) 130– 138.
- [3] K.S. Prakash, P. Balasundar, S. Nagaraja, P.M. Gopal, Mechanical and wear behaviour of Mg – SiC – Gr hybrid composites, *J. Magnes. Alloy.* 4 (2016) 197–206. doi:10.1016/j.jma.2016.08.001
- [4] I. B. Singh, M. Singh, and S. Das, A comparative corrosion behavior of Mg, AZ31 and AZ91 alloys in 3. 5 % NaCl solution, *J. Magnes. Alloy*, 3(2015), 1–7.
- [5] A. Das and S. I. P. Harimkar, Effect of Graphene Nanoplate and Silicon Carbide Nanoparticle Reinforcement on Mechanical and Tribological Properties of Spark Plasma Sintered Magnesium Matrix Composites, *J. Mater. Sci. Technol.*, 30(2014), 1059–1070,
- [6] M. Rashad, F. Pan, H. Hu, M. Asif, S. Hussain, and J. She, Enhanced tensile properties of magnesium composites reinforced with graphene nanoplatelets, *Mater. Sci. Eng. A*, 630(2015), 36–44.
- [7] S. Jothi, T. Sebald, H.M. Davies, E.D. Reese, S.G.R. Brown, "Localized microstructural characterization of a dissimilar metal electron beam weld joint form an aerospace components", *Materials & Design* 90(2016), pp.101-114.
- [8] S. Jothi, T.N. Croft, L. Wright, A. Turnbull, S.G.R. Brown, "Multi-phase modelling of intergranular hydrogen segregation/trapping for hydrogen embrittlement", *International Journal of Hydrogen Energy*, 40 (2015), pp. 15105-15123.
- [9] S. Jothi, T.N. Croft, S.G.R. Brown, "Multiscale multiphysics model for hydrogen embrittlement in polycrystalline nickel", *J. Alloys Compd.*, vol. 645(2015), S500–S504.

- [10] A. R. Rajamani, S. Jothi, M. D. Kumar, S. Srikanth, M.K. Singh, G. Otero-Irurueta, D. Ramasamy, M. Data, M. Ranagarajan, "Effects of additives on kinetics, morphologies and lead-sensing property of electrodeposited bismuth films", *J. Phys. Chem. C*, (2016), 120 (39), pp. 22398-22406.
- [11] S. Jothi, S.V. Merzlikin, T.N. Croft, J. Andersson, S.G.R. Brown, "An Investigation of micro-mechanism in hydrogen induced cracking in nickel-based superalloy 718", *J. Alloys Compd.*, vol. 664(2016), 664–681.
- [12] S. Jothi, T.N. Croft, S.G.R. Brown, "Modelling the influence of microstructural morphology and triple junctions on hydrogen transport in nanopolycrystalline nickel," *Composites Part B: Engineering*, vol. 75, (2015), pp. 104-118.
- [13] S. Jothi, T.N. Croft, S.G.R. Brown, E.A. de Souza Neto, "Finite element microstructural homogenization techniques and intergranular, intragranular microstructural effects on effective diffusion coefficient of heterogeneous polycrystalline composite media, *Composite Structures*, vol. 108 (2014), pp.555-564.
- [14] S. Jothi, T.N. Croft, S.G.R. Brown, "Meso-microstructural computational simulation of the hydrogen permeation test to calculate intergranular, grain boundary and effective diffusivities, *J. Alloys Compd.*, vol. 645(2015), S247–S251.
- [15] N. Palaniappan, L. R. Chowhan, S. Jothi, I.G. Bosco, Ivan S. Cole, "Corrosion inhibition on mild steel by phosphonium salts in 1 M HNO₃ aqueous medium", *Surfaces and Interfaces*, (2016), InPress
- [16] S. Jothi, T.N. Croft, S.G.R. Brown, "Coupled macroscale-microscale model for hydrogen embrittlement on polycrystalline materials", *International Journal of Hydrogen Energy*, vol. 40 (2015), pp.2882-2889.
- [17] S. Jothi, T.N. Croft, S.G.R. Brown, "Influence of grain boundary misorientation on hydrogen embrittlement in bi-crystal nickel", *International journal of Hydrogen Energy*, vol. 39 (2014), pp.20671-20688.
- [18] M. H. Fini and A. Amadeh, "Improvement of wear and corrosion resistance of AZ91 magnesium alloy by applying Ni – SiC nanocomposite coating via pulse electrodeposition, *Trans. Nonferrous Met. Soc. China*, 23(2013), 2914-2922.
- [19] P. Shi, B. Niu, E. Shanshan, Y. Chen, and Q. Li, "Preparation and characterization of PLA coating and PLA / MAO composite coatings on AZ31 magnesium alloy for improvement of corrosion resistance," *Surf. Coat. Technol.*, 262(2015), 26–32.
- [20] Y Fengxia Wua, Jun Lianga, Weixue Lib, "Electrochemical deposition of Mg(OH)₂/GO composite films for corrosion protection of magnesium alloys, *J. Magnes. Alloy*, 3(2015), 231-236.

- [21] S. Wang, N. Si, Y. Xia, and L. Liu, Influence of nano-SiC on microstructure and property of MAO coating formed on AZ91D magnesium alloy, *Trans. Nonferrous Met. Soc. China*, 25(2015), 1926–1934.
- [22] J.M. Hu, J.Q. Zhang, C.N. Cao, Determination of water uptake and diffusion of Cl⁻ ion in epoxy primer on aluminum alloys in NaCl solution by electrochemical impedance spectroscopy, *Prog. Org. Coat.* 46 (2003) 273–279.
- [23] Vazquez-Arenas, T. Treeratanaphitak, M. Pritzker, Formation of Co–Ni alloy coatings under direct current, pulse current and pulse-reverse plating conditions, *Electrochim. Acta* 62 (2012) 63–72.
- [24] F. Su, C. Liu, J. Guo, P. Huang, Characterizations of nanocrystalline Co and Co/MWCNT coatings produced by different electrodeposition techniques, *Surf. Coat. Technol.* 217 (2013) 94–104.
- [25] C. Fu, G. Zhao, H. Zhang, and S. Li, Evaluation and Characterization of Reduced Graphene Oxide Nanosheets as Anode Materials for Lithium-Ion Batteries, *Int. J. Electrochem. Sci.*, 8 (2013) 6269 – 6280.
- [26] H. A. Becerril, J. Mao, Z. Liu, R. M. Stoltenberg, Z. Bao, and Y. Chen, Evaluation of Solution-Processed Reduced Graphene Oxide Films as Transparent Conductors, *ACS Nano*, 2(2008), 463–470.
- [27] H. Mindivan, A. . Efe, A. H. . Kosatepe, and E. S. . Kayali, Fabrication and characterization of carbon nanotube reinforced magnesium matrix composites, *Appl. Surf. Sci.* 318(2014), 234–243.
- [28] H. He, C. Gao, General approach to individually dispersed, highly soluble, and conductive graphene nanosheets functionalized by nitrene chemistry, *Chem. Mater.* 22 (2010) 5054–5064.
- [29] V. Kavimani, K. Soorya Prakash, Titus Thankachan, Surface characterization and specific wear rate prediction of r-GO/AZ31 composite under dry sliding wear condition, *j.surfin* 6,(2017) 143-153 ,10.1016/j.surfin.2017.01.004
- [30] D. Prasai, J. C. Tuberquia, R. R. Harl, G. K. Jennings, and K. I. Bolotin, Graphene: Corrosion-inhibiting coating, *ACS Nano*, 6(2012), 1102–1108.
- [31] Y.P. Hsieh, M. Hofmann, K.W. Chang, J.G. Jhu, Y.Y. Li, K.Y. Chen, C.C. Yang, W.S. Chang, L.C. Chen, Complete Corrosion Inhibition through Graphene Defect Passivation, *ACS Nano*, 8 (2014), 443-448.
- [32] S. Chen, L. Brown, M. Levendorf, W. Cai, S. Ju, J. Edgeworth, R. S. Ruoff, and C. E. T. Al, Oxidation Resistance of Graphene- Coated Cu and Cu / Ni Alloy, *ACS nano* ,2(2011),1321–1327.

- [33] C. M. P. Kumar, T. V Venkatesha, and R. Shabadi, Preparation and corrosion behavior of Ni and Ni – graphene composite coatings, *Mater. Res. Bull.*, 48(2013),1477–1483.
- [34] D. Kang, J. Y. Kwon, H. Cho, J. Sim, H. S. Hwang, and C. S. Kim, Oxidation resistance of iron and copper foils coated with reduced graphene oxide multilayers. *ACS Nano*. 6(2012) 7763–7769
- [35] X. Zhang, Y. An, J. Han, W. Han, G. Zhao, and X. Jin, Graphene nanosheet reinforced ZrB₂ – SiC ceramic composite by thermal reduction of graphene oxide, *RSC Adv.*, 5(2015), 47060–47065.
- [36] M. Selvam, K. Saminathan, P. Siva, P. Saha, and V. Rajendran, “Corrosion behavior of Mg / graphene composite in aqueous electrolyte,” *Mater. Chem. Phys.*, pp. 1–8, 2016.
- [37] Peng Wang, Tao Yao, Bo Sun, Xiaoliang Fan, Sijie Dong, Yun Bai, Yu Shi “A cost-effective method for preparing mechanically stable anti-corrosive superhydrophobic coating based on electrochemically exfoliated graphene” *J. Colloid Interface Sci.*, 513(2017)396-401
- [38] Cheng Chen, , Shihui Qiu, , Mingjun Cui, , Songlv Qin, , Songlv Qin, , Haichao Zhao, , Liping Wang, , Qunji Xue “Achieving high performance corrosion and wear resistant epoxy coatings via incorporation of noncovalent functionalized graphene”, *Carbon* 114 (2017) 356-366
- [39] C.F. Glover, , C. Richards, , J. Baker, , G. Williams, , H.N. McMurray, “In-coating graphene nano-platelets for environmentally-friendly corrosion protection of iron” *Corros. Sci.*, 114 (2017) 169–172
- [40] Jingmao Zhao , Xiong Xie, , Chen Zhang, “Effect of the graphene oxide additive on the corrosion resistance of the plasma electrolytic oxidation coating of the AZ31 magnesium alloy” *Corros. Sci.*, 114 (2017) 146–155
- [41] C. Zhang, S. Pei, H. Ji, , Y. Cui ,M. Li, “Fabrication of Ni60–SiC coating on carbon steel for improving friction, corrosion properties” *Mat. Sci. & Tech.* (2016)1-8
- [42] Zhonghua Xuea, Bo Yina,1, Mengqian Lia,, Honghong Raob, Hui Wanga, Xibin Zhoua, Xiuhui Liua, Xiaoquan Lua, “Direct electrodeposition of well dispersed electrochemical reduction graphene oxide assembled with nickel oxide nanocomposite and its improved electrocatalytic activity toward 2, 4, 6-Trinitrophenol” *Electrochim. Acta* 192 (2016) 512–520
- [43] Hadi Nasiri Vatan, Reza Ebrahimi Kahrizsangi, Masoud Kasiri Asgarani, “Growth, Corrosion and Wear Resistance of SiC Nanoparticles Embedded MAO Coatings on AZ31B Magnesium Alloy” , *Prot Met Phys Chem Surf*, 52(2016) 859–868.

- [44] Swarnima Singh, M. Sribalaji, Nitin P. Wasekar, Srikant Joshi, G. Sundararajan, Raghuvir Singh, Anup Kumar Keshri, "Microstructural, phase evolution and corrosion properties of silicon carbide reinforced pulse electrodeposited nickel–tungsten composite coatings" *Appl. Surf. Sci.* 364 (2016) 264–272
- [45] Jayanta Mondal, Jekaterina Kozlova, and Väino Sammelselg, "Graphene Nanoplatelets Based Protective and Functionalizing Coating for Stainless Steel" *J Nanosci Nanotechnol*, 15(2015)6747–6750
- [46] B. Mingoa, R. Arrabal, M. Mohedano, A. Pardo, E. Matykina, "Corrosion and wear of PEO coated AZ91/SiC composites" *Surf. Coat. Technol.*, 309(2017)1023-1032
- [47] W.S. Hummers and R.E. Offeman, *J. Am. Chem. Soc.*, 80 (1958) 1339.
- [48] A. B. Ikhe, A. B. Kale, J. Jeong, M. J. Reece, S.-H. Choi, and M. Pyo, "Perfluorinated polysiloxane hybridized with graphene oxide for corrosion inhibition of AZ31 magnesium alloy," *Corros. Sci.*, (2016) pp. 1–8.
- [49] Y. Bai, Y. Bai, J. Gao, W. Ma, J. Su, and R. Jia, "Preparation and characterization of reduced graphene oxide / fluorhydroxyapatite composites for medical implants," *J. Alloys Compd.*, vol. 688, (2016.) pp. 657–667,
- [50] N. A. Kumar, H. Choi, Y. R. Shin, D. W. Chang, and L. Dai, "Polyaniline-Grafted Reduced Graphene Oxide for Efficient Electrochemical," *ACS nano* 2, pp.(2012) 1715–1723.
- [51] M. C. Turhan, Q. Li, H. Jha, R. F. Singer, and S. Virtanen, "Corrosion behaviour of multiwall carbon nanotube/magnesium composites in 3.5% NaCl," *Electrochim. Acta*, vol. 56, no. 20, (2011) pp. 7141–7148.
- [52] M. Stern, A. Geary, *J. Electrochem. Soc.* 104 (1957) 56
- [53] L. Shi, C. Sun, P. Gao, F. Zhou, and W. Liu, Mechanical properties and wear and corrosion resistance of electrodeposited Ni – Co / SiC nanocomposite coating, *Appl. Surf. Sci.* 252(2006), 3591–3599.
- [54] C. M. P. Kumar, T. V. Venkatesha, and R. Shabadi, "Preparation and corrosion behavior of Ni and Ni-graphene composite coatings," *Mater. Res. Bull.*, vol. 48, no. 4, (2013) pp. 1477–1483,
- [55] B. P. Singh, S. Nayak, K. K. Nanda, B. K. Jena, S. Bhattacharjee, and L. Besra, "The production of a corrosion resistant graphene reinforced composite coating on copper by electrophoretic deposition," *Carbon N. Y.*, 2013.
- [56] N. M. Kumar, S. S. Kumaran, and L. A. Kumaraswamidhas, An investigation of mechanical properties and corrosion resistance of Al2618 alloy reinforced with Si₃N₄,

AlN and ZrB₂ composites, J. Alloys Compd., vol. 652(2015),244–249.

- [57] S. A. McCluney, S. N. Popova, B. N. Popov, R. E. White and R. B. Griffin, "Comparing Electrochemical Impedance Spectroscopy Methods for Estimating the Degree of Delamination of Organic Coatings on Steel" 139(1992), 1556-1560